Medieval Arch Bridges in the Lanzo Valleys, Italy: Case Studies on Incremental Structural Analysis and Fracturing Benefit

Federico Accornero[1]; Giuseppe Lacidogna[2]; and Alberto Carpinteri, F.ASCE[3]

Abstract: After presenting a historical overview concerning the masonry arch design, this article proposes a computational procedure that allows the capture of the arch-damaging process, which takes place when the conditions assessed through linear elastic analysis are no longer valid and before the set-in of the conditions established by means of limit analysis. This evolutionary analysis of the fracturing process is then applied to three medieval masonry arch bridges located in the Lanzo Valleys (Italy). Through damage assessment, the present work shows how the arch thrust line is affected by crack formation and the internal stress redistribution; it also shows that the maximum admissible load evaluated by means of linear elastic fracture mechanics is greater than the load predicted by the theory of elasticity. Such an increment in terms of maximum admissible load can be defined as the fracturing benefit, and it is analogous to the plastic benefit of limit analysis. **DOI: 10.1061/(ASCE)BE.1943-5592.0001252.** © *2018 American Society of Civil Engineers.*

Author keywords: Masonry structures; Masonry arches; Evolutionary fracture analysis; Fracturing benefit; Mery's method.

Introduction and Historical Overview

Over the centuries, different critical approaches have been used to address the problem of masonry arch design methods (Benvenuto and Radelet de Grave 1995; Betti et al. 2008; Karnowsky 2012; Lacidogna and Accornero 2018; Page 1993; Poncelet 1852). These approaches are briefly described in chronological order to show how the partial understanding of arch structural behavior, as can be acquired from traditional methods, might be effectively improved. Such improvement can be represented by an elastic-softening constitutive law that takes into account the possibility of crack formation in the arch structure during its life (Accornero et al. 2016; Carpinteri and Carpinteri 1982, Carpinteri et al. 2015).

In the present work, a linear elastic fracture mechanics (LEFM) numerical procedure concerning masonry arches is first outlined, and then an application of the evolutionary analysis of the fracturing process to three monumental arch bridges dating back to the Middle Ages is presented. Here, the results obtained by the LEFM model are compared with the outcomes of a linear elastic model, in particular, the Mery's method. In the last section, the fracturing benefit found by means of LEFM is presented as a gradual transition from an elastic stage of the structure to a completely damaged one that involves the ultimate bearing capacity of the arch according to limit analysis.

[1]Research Assistant, Dept. of Structural Geotechnical and Building Engineering, Politecnico di Torino, Corso Duca degli Abruzzi 24, Torino 10129, Italy (corresponding author). E-mail: federico.accornero@polito.it

[2]Associate Professor, Dept. of Structural Geotechnical and Building Engineering, Politecnico di Torino, Corso Duca degli Abruzzi 24, Torino 10129, Italy.

[3]Full Professor, Dept. of Structural Geotechnical and Building Engineering, Politecnico di Torino, Corso Duca degli Abruzzi 24, Torino 10129, Italy.

Note. This manuscript was submitted on September 13, 2017; approved on January 8, 2018; published online on May 11, 2018. Discussion period open until October 11, 2018; separate discussions must be submitted for individual papers. This paper is part of the ***Journal of Bridge Engineering***, © ASCE, ISSN 1084-0702.

The following discussion proposes a timeline subdivision of the scientific periods relating to masonry arch design.

Geometric and Empirical Design

For several centuries, methods that relied exclusively on geometric parameters were used to provide dimension to vaulted structures (Vitruvius Pollio 1914; Vittone 1766). If, on the one hand, such methods originated from experience and provided an answer to the static problem, on the other, they neglected the intrinsic mechanisms forming the basis of the phenomena observed (Fig. 1).

Among the empirical approaches, we have to recall the statement given by Robert Hooke in 1675, who, at the end of his treatise on helioscopes (Hooke 1675), wrote: "*Ut pendet continuum flexile, sic stabit contiguum rigidum inversum*," which translates as, "As hangs the flexible line, so but inverted will stand the rigid arch" (Fig. 2). This sentence, originally written as an anagram (Heyman 1998; Hooke 1675), generalizes the idea of the funicular shape that a string takes under a set of loads. If rigidified and inverted, this shape illustrates a path of compressive forces for an arched structure to support the same set of inverted loads (Block et al. 2006; Poleni 1748).

Early Kinematic Approach

In the eighteenth century, design, as it is meant today, saw the light, thanks to De La Hire (1730) and Mascheroni (1785), among others, who performed theoretical analyses and experimental tests to assess the state of an arch at final collapse. The developed design philosophy is close to the notions underlying both modern limit state and plastic design (Fig. 3).

A significant contribution to the developing of De La Hire's topics was provided by Claude Antonie Couplet. He introduced the concepts of *engrenèment entre les voussoir*, that is, adherence and friction, which prevent the sliding along joints, and *charnières*, that is, the hinges whose formation allows the mutual rotation of the blocks (Couplet 1731). Couplet's work, albeit little known among

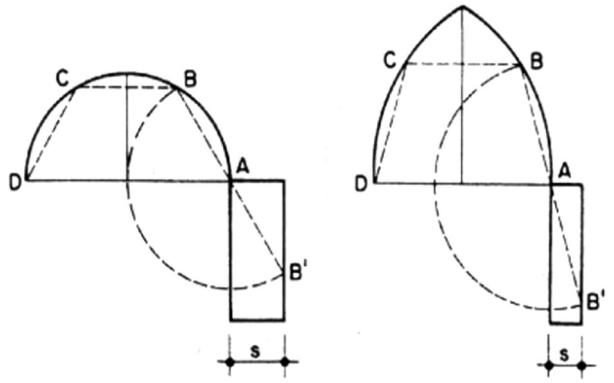

Fig. 1. Empirical formula for arch design: $\overline{AB} = \overline{BC} = \overline{CD} = \overline{AB'}$ (adapted from Vittone 1766)

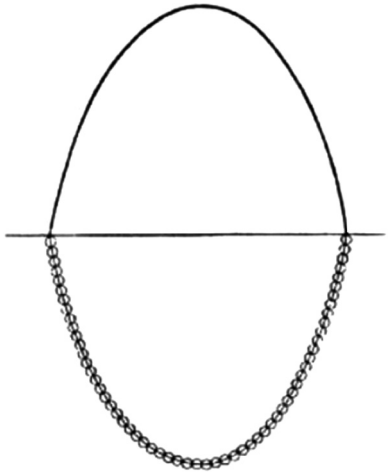

Fig. 2. Poleni's drawing of Hooke's analogy between an arch and a hanging chain (adapted from Poleni 1748)

his contemporaries, has the great merit of expressing an outstanding progression in the theoretical setting of structural mechanics (Becchi and Foce 2002; Paradiso et al. 2007).

It is quite singular to note that the contribution given by Couplet was almost ignored in the following years. In fact, in 1773 Coulomb presented to the French Royal Academy the concepts of friction and hinge between arch blocks as absolutely original aspects (Coulomb 1773). However, Coulomb disseminated in a comprehensive and clear way the need to consider friction and sliding to address the problem of masonry arch design.

Elastic Analysis

Navier (1833) was the first to observe the distribution of stresses at the interfaces between arch segments accurately. He shifted the focus of the analysis to the actual state of stress in the material. To analyze stress distribution over a cross section, he introduced the thrust-line concept (Lacidogna and Accornero 2018). He also proved that the resulting line of action must lie within the central kern to prevent tension (Navier 1833).

Mery's (1840) studies gained widespread recognition. They were extensively used in the dimensioning of arch structures. His method was based on the use of a graphing procedure to check the thrust line in agreement with the stress limitations identified by Navier (Mery 1840).

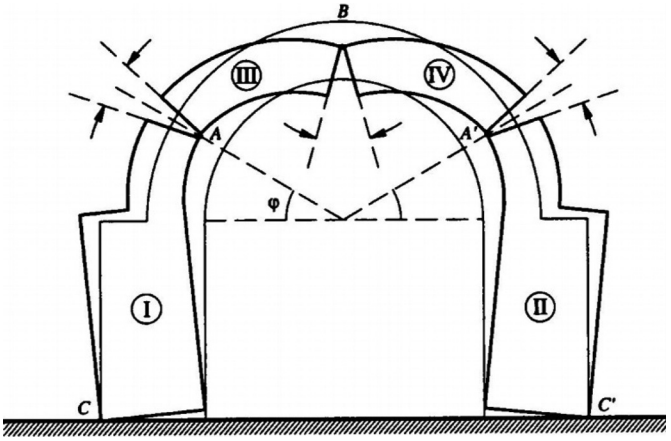

Fig. 3. Arch-collapse mechanism consisting of four rigid blocks (I, II, III, IV) with two external hinges (in C and C′) and three internal hinges (in A, A′, and B) (adapted from Mascheroni 1785)

Soon, the application of the theory of elasticity encountered criticism: The concepts of homogeneity and isotropy, in fact, were far from the real conditions of damaged and cracked materials.

Alberto Castigliano (1879) tackled the problem by applying the minimum strain energy theorem to masonry arches (Castigliano 1879; Carpinteri et al. 2015). He also introduced the concept of an elastically imperfect system: "*Les corps qui, après avoir été comprimés, ne reprennent pas exactement leur formes primitives en enlevants les forces extérieurs*."

Modern Kinematic Approach (Limit Analysis)

The rigid-block model used in the eighteenth century to study the behavior of masonry arches underwent major revisions during the last century as a result of the various experiments carried out on arch models (Page 1993; Pippard 1948). One of the most significant revisions with respect to the eighteenth-century theories was formulated by Heyman (1966, 1982). Referring back to Kooharian's (1953) studies, he proposed to systematically apply the plastic analysis theorems to the issue of the stability of masonry arches in kinematic terms. He introduced three basic assumptions for such application: "stone has no tensile strength; stone has infinite compressive strength; the sliding of a stone on another cannot occur."

The choice of this constitutive law for the material, however, seems to be penalizing compared to the way the material actually behaves. In fact, although it may be true that the shear component of the stress, exerted between two adjacent voussoirs, cannot by any means exceed the friction resistance, the fact remains that stone is considered as a material with no tensile strength but infinite compressive strength.

Starting from these assumptions, the formation of a hinge right where the thrust line is tangent to the arch at the edges can be acknowledged; thus, a rigid rotation of the faces of the two adjacent segments takes place around the extreme fiber of the section (Gilbert and Melbourne 1994).

Three tangential points lead to the formation of three hinges; this results in a statically determinate structure. The limit to trigger a kinematic collapse mechanism lies in the formation of a fourth hinge. The limit analysis consists of the identification of the lowest possible load multiplier that generates a line of thrust that is always contained within the arch volume and tangential to arch edges at four points (hinges) (Fig. 4).

Recent Developments

Extensive studies have been carried out recently on arch and vault structures (Boothby 2001; Casapulla 2001; Casapulla and Argiento 2016; Drosopoulos et al. 2006; Orduña and Lourenço 2005; Tóth et al. 2009), some of them dealing with the problem of friction resistance. Several studies based on the finite-element method (FEM) and on nonlinear FEM tension models (Milani and Lourenço 2012) show the potential of the method to compute both load-deflection curves and the interaction of the arch structure with the filling (Cavicchi and Gambarotta 2007). In particular, it is worth noting that the nonlinear tensile behavior models used in finite-element analysis stem directly from fracture mechanics theories.

Finally, more recent methods (Carpinteri et al. 2015; Accornero et al. 2016; Lacidogna and Accornero 2018) for the evaluation of masonry arch structure stability consist of incremental analysis of the fracturing process by means of LEFM.

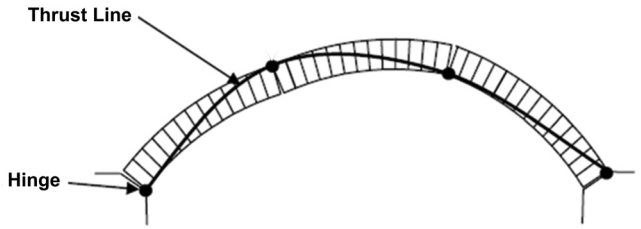

Fig. 4. Four-hinge arch-collapse mechanism (adapted from Heyman 1982)

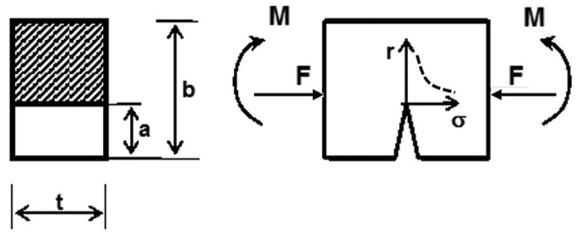

Fig. 5. Cracked beam element: (a) $\xi = a/b$; (b) $\sigma = K_I(2\pi r)^{-0.5}$

LEFM Model for Masonry Arches

The elastic-softening constitutive law best representing masonry behavior (Carpinteri and Carpinteri 1982; Lourenço 2000) corresponds to simply considering an elastic constitutive law associated with a fracturing condition consistent with the concepts of LEFM. This means that the material has a merely elastic behavior with the possibility that cracks might form and propagate (Carpinteri and Carpinteri 1982; Carpinteri et al. 2015; Carpinteri and Accornero 2018).

The relative crack depth $\xi = a/b$ [Fig. 5(a)] and the stress intensity factor K_I [Fig. 5(b)] are taken into consideration as the damage parameter and load parameter, respectively. The Mode I stress intensity factor is a stress field's amplification factor when the loads are symmetrical to the crack (e.g., axial force and bending moment) (Carpinteri 1982; Tada et al. 1985).

Shear is disregarded. The validity of this assumption, taking into account Mery's method (Mery 1840) and the Heyman hypotheses of limit analysis (Heyman 1982), can be verified by considering the slope of the arch thrust line with respect to the joint lines. If the thrust line affects the joints with a slope less than the angle of friction, no mutual sliding takes place between two adjacent elements (Fett 2001). Also, from a LEFM point of view, the presence of the compressive stresses in the arch structure reduces the risk of Mode II failure (shear).

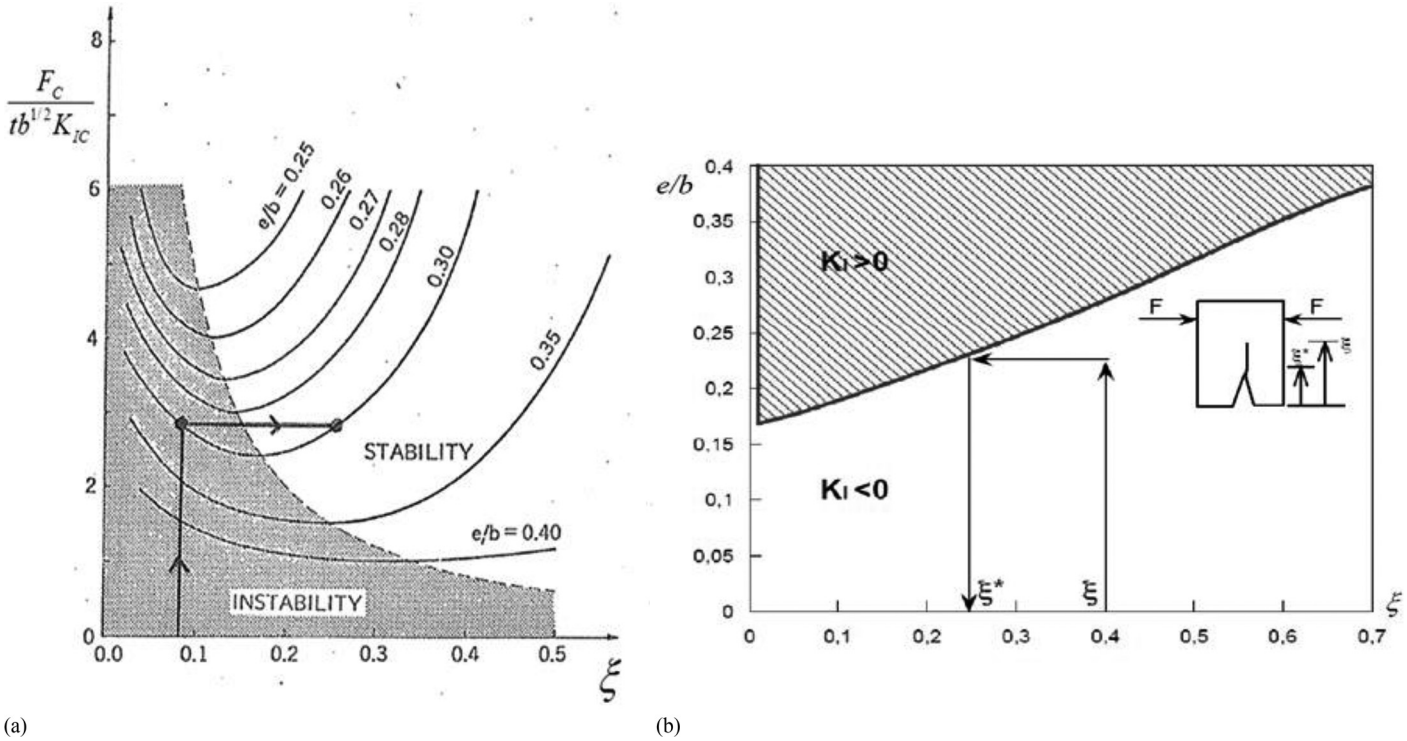

(a) (b)

Fig. 6. Fracturing process for off-center compression: (a) snap-through instability; (b) crack closure curve

With a compressive axial force, and when the bending moment opens the crack (Fig. 5), as is usually the case with masonry arches, it is possible to determine the total stress intensity factor by means of the superposition principle (Carpinteri et al. 2015):

$$K_I = K_{IM} - K_{IF} = \frac{M}{tb^{3/2}} Y_M(\xi) - \frac{F}{tb^{1/2}} Y_F(\xi) = \frac{F}{tb^{1/2}} \left[\frac{e}{b} Y_M(\xi) - Y_F(\xi) \right] \quad (1)$$

where K_{IM} = stress intensity factor attributable to the bending moment $M = Fe$; K_{IF} = stress intensity factor for the compressive axial force F; and e = eccentricity of the axial force, relating to the cross-sectional area centroid. The algebraic minus sign in Eq. (1), based on the superposition principle, is attributable to the effect of the compressive axial force that tends to close the crack, whereas the bending moment opens the crack. Moreover, as noted by Tada et al. (1985), $Y_M(\xi)$, $Y_F(\xi)$ represent the shape functions for K_{IM} and K_{IF}, respectively.

The critical condition $K_I = K_{IC}$ allows determining the relation between two parameters: on the one hand, the dimensionless crack extension axial force as a function of crack depth ξ; on the other, the load's relative eccentricity, e/b:

$$\overline{F}_c = \frac{F_C}{tb^{1/2} K_{IC}} = \frac{1}{\frac{e}{b} Y_M(\xi) - Y_F(\xi)} \quad (2)$$

Fig. 7. Forno di Lemie Bridge (image by Federico Accornero)

Table 1. Mechanical Characteristics of Serpentinite Stone

Characteristic	Value
Unit weight γ (kN/m^3)	27.00
Young's modulus E (MPa)	55,000.00
Compressive strength σ_c (MPa)	75.00
Tensile strength σ_t (MPa)	5.00
Fracture toughness K_{IC} (N/mm$^{3/2}$)	32.00

Eq. (2) is graphically represented by the curves in Fig. 6(a), which also show how, with a fixed eccentricity e/b, the fracturing process becomes stable only after an unstable crack propagation. If the load F does not follow the decreasing unstable branch in strain-softening unloading processes along an e/b = constant curve, then the fracturing process will show a catastrophic behavior: The representative point will advance horizontally until again meeting the e/b = constant curve and will be situated on the stable branch (snap-through instability). Moreover, the possibility of load relaxation and the possibility of a less catastrophic fracturing behavior are linked to structural geometry and mechanical characteristics. The occurrence of a snapping phenomenon is especially affected by both the degree of redundancy and the structural size (Carpinteri 1982, 1989b).

It is also important to take into account that for each relative crack depth ξ, a relative eccentricity value exists, below which the crack tends to close again, at least partially (Carpinteri et al. 2015). The closing condition $K_I = 0$, leads to

$$K_I = 0 = \frac{F}{tb^{1/2}} \left[\frac{e}{b} Y_M(\xi) - Y_F(\xi) \right] \quad (3)$$

from which

$$\frac{e}{b} = \frac{Y_F(\xi)}{Y_M(\xi)} \quad (4)$$

Fig. 6(b) graphically represents the closing condition of Eq. (4). The area below the curve represents both the crack and the loading conditions whereby $K_I < 0$. The depth ξ^*, conversely, represents the relative depth of the crack partially open.

The cracked cross-sectional behavior (Fig. 5) is similar to that of an elastic hinge whose rotational stiffness is calculated by means of the energy balance between the elastic work and the fractured one. Therefore, the cracked element's stiffness matrix is modified exclusively by the four rotational terms (Carpinteri et al. 2015).

Setting both the structure's geometrical characteristics and the material's mechanical properties, such as, for instance, the fracture toughness and the maximum compressive stress, the arch is analyzed through a FEM model in which the masonry structure is clamped to rigid abutments. The structure is subdivided into beam elements, and the corresponding applied load on the elements is considered, as is the eventual stiffness loss of the cracked beam cross section. Namely, whereas an uncracked cross section of a beam element carries out the internal action of a perfectly fixed joint, a cracked cross section carries out the internal action of an elastically fixed joint (Carpinteri and Carpinteri 1982; Carpinteri et al. 2015). Such a stiffness loss can be represented by the so-called brittle hinge (Taylor and Mallinder 1993).

The calculation routine adopts a step-by-step loading process; for each load increment, the code returns both the axial force and the bending moment relating to each section. These values, by means of the beam theory's classical relations, allow determining

Table 2. Forno Di Lemie Bridge: Incremental Analysis of the Fracturing Process (Bold Text Indicates Local Failures)

		Node 4		Node 10		Node 14	
Step	Live load (kN/m)	Relative crack depth ξ	Compressive stress σc (MPa)	Relative crack depth ξ	Compressive stress σ_c (MPa)	Relative crack depth ξ	Compressive stress σ_c (MPa)
1	0.00	0.00	2.10	0.00	2.30	0.00	2.30
2	5.40	0.00	15.80	Crack initiation	11.90	0.00	15.50
3	5.60	0.43	43.70	**0.71**	**121.50**	0.44	43.70

the maximum tensile or compressive forces and their eccentricity with regard to the centroid in each section within the structure.

When tensile stresses trigger a cross-sectional crisis, it is possible to determine the relative crack depth ξ from Eq. (2). This gives the relation between the crack depth ξ and the axial force's relative eccentricity e/b. Thus, the updated crack depth is assessed (Accornero et al. 2016; Carpinteri et al. 2015). From Eq. (2), Fig. 6(a) shows some dimensionless curves.

The routine is thus applied again, taking into account the cracked elements' modified stiffness (brittle hinge). In the case where the new relative crack depth ξ is the same as the one previously determined, the process stabilizes. In the case where the new relative crack depth ξ is lower than the former, then the routine resorts to the so-called curve of closure [see Eq. (4)], determining the admissible crack depth. After such check, only the ξ values that fall in the $K_I \geq 0$ field [see Fig. 6(b)] are taken into consideration.

By increasing the load, the arch cross section's inefficiency occurs when $\xi \geq 0.7$ (Carpinteri et al. 2015); in this case, a fracturing collapse occurs. An analogous inefficiency takes place also when the compressive strength (relating to the element taken into consideration) is reached; then, a crushing collapse occurs (Lacidogna et al. 2013).

The proposed method allows capturing the arch-damaging process, which takes place when the conditions assessed through linear

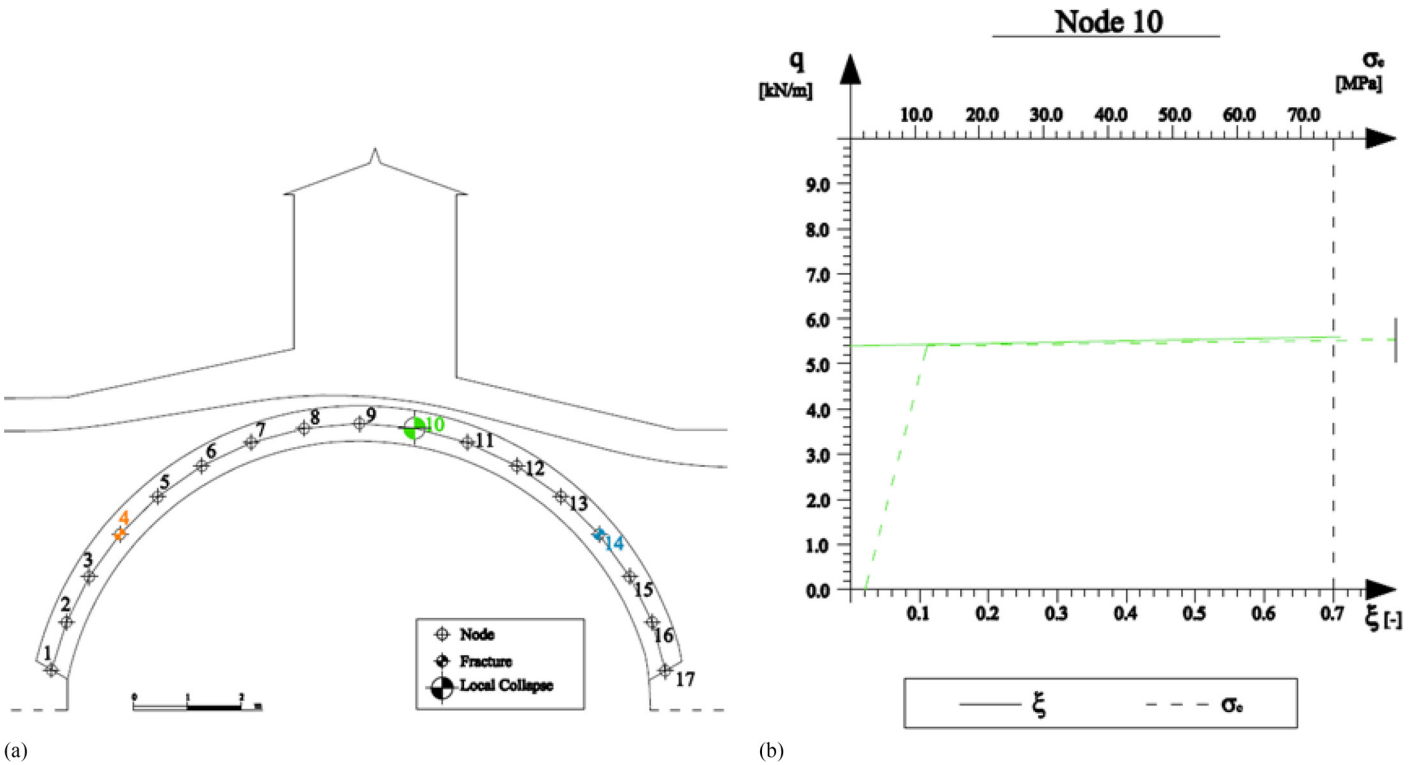

Fig. 8. Forno di Lemie Bridge: (a) damage localization; (b) local collapse

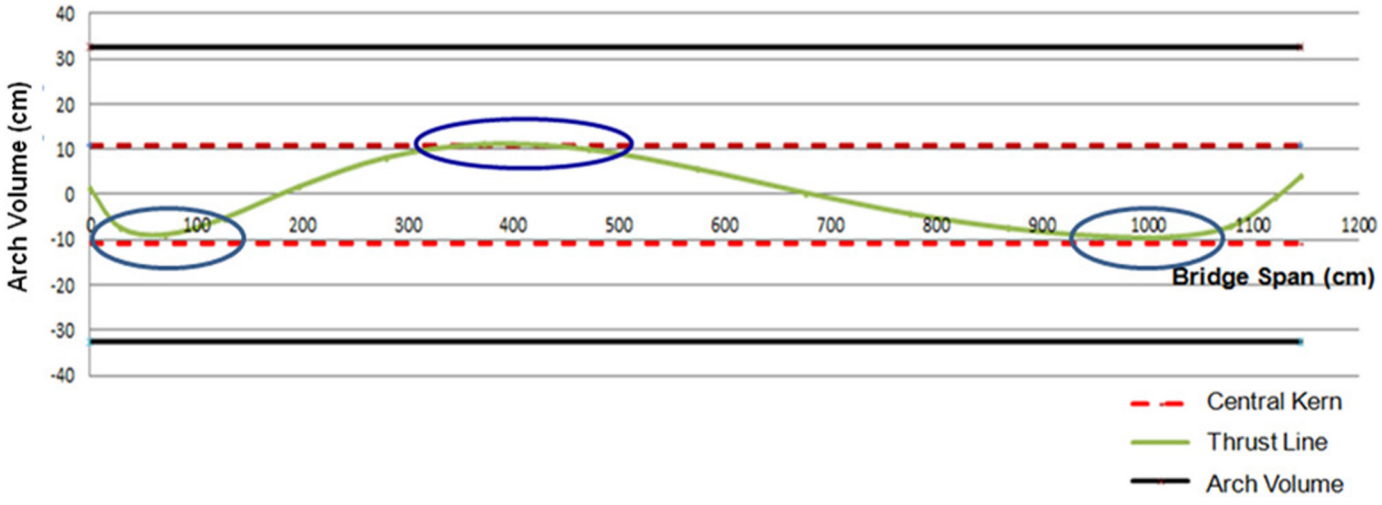

Fig. 9. Forno di Lemie Bridge analyzed by Mery's method, taking into account the dead load alone; to better appreciate the thrust-line trend, arch volume and central kern contours are rectified following Fuller's theory (adapted from Fuller 1875)

elastic analysis are no longer valid and before the set-in of the conditions established by means of the limit analysis. Therefore, the evolutionary analysis of fracturing process numerically assesses how the arch structural behavior is affected by crack formation and considers the internal stress redistribution (Accornero et al. 2016). In the following, by means of LEFM, an application of the evolutionary analysis to three monumental arch bridges dating back to the Middle Ages (Cavallari-Murat 1973) is presented. In addition, the results obtained by LEFM are compared with the outcomes of the linear elastic model (Mery's method). In general, the middle third rule (i.e., the arch cross section must be entirely compressed) does not represent a limit state assessment, and such a condition is known to be highly conservative for most arches. Nevertheless, Mery's method can still be considered a useful and effective comparison tool because it does not need a constitutive model for masonry to be defined (Brencich and Morbiducci 2007).

Moreover, in this application, concerning specifically LEFM of masonry, arch–soil interaction is neglected, as is the interaction of the structure with the filling.

Historical Masonry Arch Bridges of the Lanzo Valleys

The Lanzo Valleys are in the northwestern part of Piedmont, near Turin (Italy). The Stura di Lanzo River, a tributary of the Po River, collects the waters flowing through the valleys. During the centuries, many of these secondary rivers made it necessary to build bridges, mostly consisting of masonry arches, to allow an easy way of communication for the Lanzo Valleys inhabitants (Cavallari-Murat 1973).

This article presents a study of the fracturing process in three masonry arch bridges situated in the Lanzo Valleys: Forno di Lemie Bridge, Fucine di Viù Bridge, and the Devil's Bridge, Ponte del Roch.

Fig. 10. Fucine di Viù Bridge (image by Federico Accornero)

The Forno di Lemie Bridge (Fig. 7) leads to the homonymous village, which is characterized by silver, copper, and iron mines. The bridge is a stone arch with a canopy, once decorated with frescoes, dating back to 1477 (Cavallari-Murat 1973).

The arch structure presents a span of 11.00 m, a rise of 5.60 m, and a thickness of 0.80 m, and the arch segments are mostly constituted by serpentinite, a rock formed by hydration and metamorphic transformation of ultramafic rock from the Earth's mantle, typical of the Lanzo Valleys.

The principal mechanical characteristics of the stone arch material are reported in Table 1. The unit weight of the filling is considered to be equal to that of the arch structure. The live load is considered to be uniformly distributed.

The analysis of the fracturing process for the Forno di Lemie Bridge is summarized in Table 2, where the loading steps are associated both with the damage increase and the maximum compressive stress values in the section ligament for the nodes in which the fracturing process is occurring (brittle hinges). As shown in Table 2 and Fig. 8(b), for each load increment, the code returns the maximum compressive stress and the crack depth ξ related to each damaged section. In the double-abscissa diagram of Fig. 8(b), the upper abscissa represents the compressive stress, whereas the lower abscissa represents the relative crack depth. In the case of Forno di Lemie Bridge, the increment in loading led to an increment in compressive stresses and fracture damaging, particularly localized in certain nodes. The first loading step concerned the bridge dead load alone, including the arch filling; the whole bridge remained undamaged (no cracks), and the maximum compressive stress in the arch was equal to 2.30 MPa. After the second step, as shown in Fig. 8(b), in the cross section of Node 10, the uniformly distributed live load q = 5.40 kN/m caused crack initiation, and the maximum compressive stress acting in the ligament, σ_c, was equal to 11.90 MPa. At the third step, for a live load, q, equal to 5.60 kN/m, a local collapse for both fracturing and crushing took place at Node 10 [Fig. 8(b)], whereas at Nodes 4 and 14, two symmetrical cracks were formed, with a relative depth equal to 0.43 and 0.44, respectively. According to the incremental analysis of the fracturing process, the maximum distributed live load that triggered the local failure was equal to 5.60 kN/m, whereas when taking Mery's method (Brencich and Morbiducci 2007; Mery 1840) into account, the maximum admissible distributed live load was equal to zero. In fact, with the bridge dead load alone, and applying Mery's method, the thrust line was found to fall outside the arch section central kern in three points (Fig. 9).

Moreover, according to fracture evolutionary analysis, the increase in terms of maximum admissible load can be defined as the fracturing benefit, and it is analogous to the plastic benefit of limit analysis [Accornero et al. 2016; Heyman 1966, 1982; Lacidogna and Accornero 2018). In more general terms, a comparison can arise between the aforementioned fracturing benefit and the ductile-to-brittle transition observed in damaged solids (Carpinteri 1989a, b). As a matter of fact, in a displacement-controlled loading process, an

Table 3. Fucine Di Viù Bridge: Incremental Analysis of the Fracturing Process (Bold Text Indicates Local Failures)

		Node 3		Node 4		Node 9		Node 15	
Step	Live load (kN/m)	Relative crack depth ξ	Compressive stress σ_c (MPa)	Relative Crack depth ξ	Compressive stress σc (MPa)	Relative crack depth ξ	Compressive stress σ_c (MPa)	Relative crack depth ξ	Compressive stress σ_c (MPa)
1	0.00	0.00	1.00	0.00	9.00	0.00	0.70	0.00	1.00
2	4.20	0.34	36.30	0.00	13.70	0.32	24.40	0.34	35.60
3	5.20	0.35	45.50	0.34	41.00	0.41	42.00	0.34	43.40
4	5.60	0.35	46.60	0.34	41.90	0.41	46.40	0.35	47.10
5	7.40	0.35	61.40	0.34	55.00	0.42	63.50	0.35	59.70
6	9.20	0.35	**76.50**	0.34	69.20	0.42	**76.40**	0.35	73.50

almost-undamaged structural element may present brittle behavior in the post-peak branch, whereas a comparatively more damaged one can be ductile; a damaged ligament can avoid snap-back instabilities, presenting a post-peak softening response (Carpinteri and Accornero 2018). In the case of incremental analysis of the fracturing process, the damage increase induces a structural behavior better than the one described by the classical theory of elasticity.

The second masonry arch bridge analyzed in this article is the Fucine di Viù Bridge (Fig. 10). This stone humpback bridge on the Viana River is supposed to have been built after 1469, when a terrible flood destroyed 13 bridges and 10 forges in the Lanzo Valleys, inducing the Duke Amedeo IX of Savoy to exempt Lanzo Valleys from any form of tribute for 10 years (Cavallari-Murat 1973).

The arch structure presents a span of 14.90 m, a rise of 3.80 m, and a thickness of 0.70 m. The material constituting the arch segments is similar to that of the Forno di Lemie Bridge.

The analysis of the fracturing process for the Fucine di Viù Bridge is summarized in Table 3. In this case, the incremental analysis of the fracturing process involved a crack closure phenomenon, as theoretically described previously, localized at Nodes 3 and 9 [Fig. 11(b)]. As in the previous case, in the double-abscissa diagram of Figure 11(b), the upper abscissa represents compressive stresses, whereas the lower abscissa represents the relative crack depth. The first loading step involved the bridge dead load alone, including the arch filling (see Table 3); the bridge remained undamaged. After the second step, four symmetrical cracks formed at Nodes 3, 4, 9, and 15, and two significant crack closures occurred at Nodes 3 and 9 [Fig. 11(b)]. At the sixth step, two local collapses for crushing took place at Nodes 3 and 9 [Fig. 11(b)], for a maximum distributed live load equal to 9.20 kN/m. On the contrary, taking Mery's method into account, the maximum admissible distributed live load was found to be equal to zero. Also in this case, with the bridge

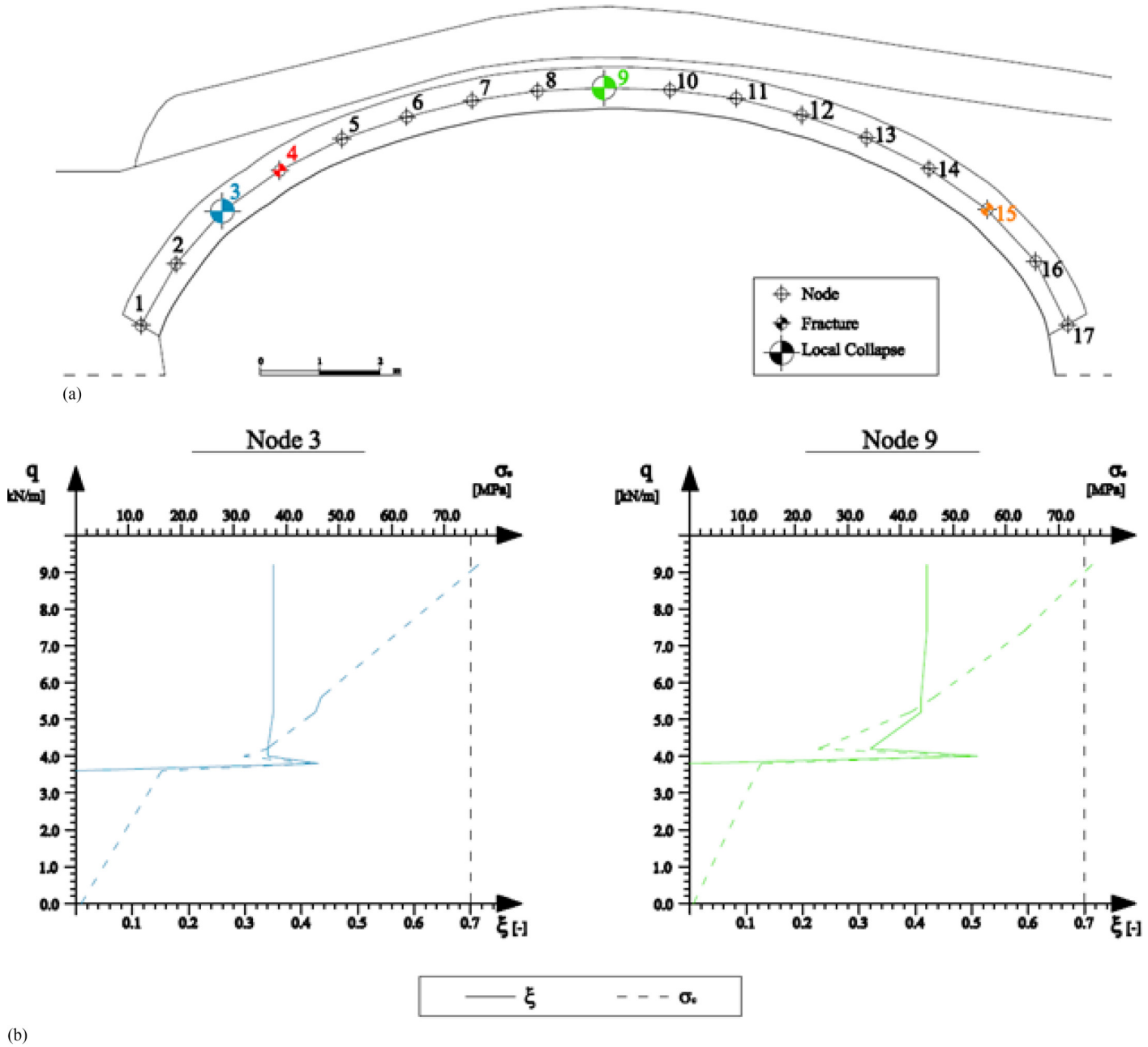

Fig. 11. Fucine di Viù Bridge: (a) damage localization; (b) local collapses

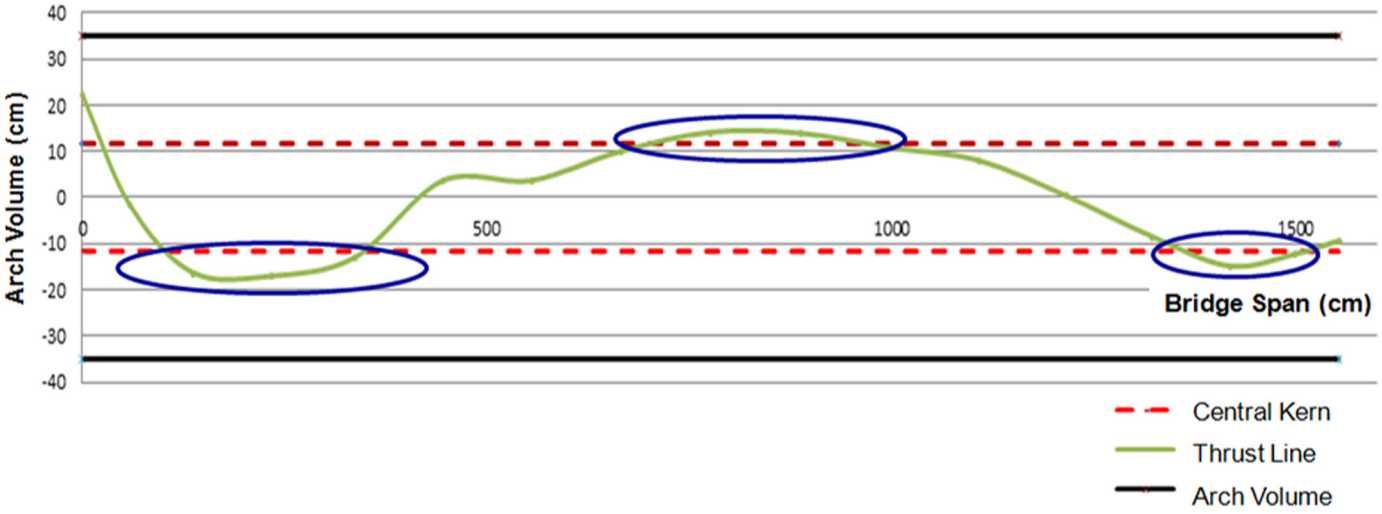

Fig. 12. Fucine di Viù Bridge analyzed by Mery's method, taking into account the dead load alone; to better appreciate the thrust-line trend, arch volume and central kern contours are rectified following Fuller's theory (adapted from Fuller 1875)

dead load alone, and applying Mery's method, the thrust line fell outside the arch section central kern in three points (Fig. 12). A consistent fracturing benefit (Accornero et al. 2016) can be found by applying the incremental analysis of the fracturing process.

The last masonry arch bridge analyzed in this article is the Devil's Bridge, Ponte del Roch (Fig. 13). On June 1, 1378, the lord of the region, Aresmino Provana, decided to create this bridge and impose a 10-year toll on wine. The bridge, overcoming torrent Stura, is 35.10 m in span, and it is formed by one arch structure 14.20 m high, with a thickness of 1.35 m. It is a humpback bridge of great architectural and historical value.

Popular imagination indulged itself in creating legends around the bridge, to the extent that it was ascribed to the devil. Some even point out, at the beginning of the bridge, the footprint left by the devil's claw; as a matter of fact, after finishing the job, the devil would have had to cross the bridge with one big step only. Others see it as a sign of the devil's anger because of the trick by the people of Lanzo Valleys who, instead of a soul as agreed, left him a cheese round (Cavallari-Murat 1973).

The analysis of the fracturing process for the Devil's Bridge, Ponte del Roch, leads to the following results. As shown in Table 4 and in Figure 14(b), after the second loading step, one crack formed at Node 8, whereas at the third step, a local collapse in Node 8 for both fracturing and crushing was triggered [Fig. 14(b)], with a snap-through instability in the cross section for a relative eccentricity $e/b = 0.40$ [Fig. 14(c)]. The maximum distributed live load that set off the local failure (fracturing benefit) was equal to 2.80 kN/m, whereas when taking Mery's method into account, the maximum admissible distributed live load was equal to zero (Fig. 15), as in the previous cases. Therefore, a fracturing benefit can be found by means of LEFM. In addition, the fact that the shape of the Devil's Bridge involves a small filling action at the springs can be considered as one of the causes for the comparatively poor load-carrying capacity shown by the arch structure.

Fig. 13. Devil's Bridge, Ponte del Roch (image by Federico Accornero)

Table 4. Devil's Bridge: Incremental Analysis of the Fracturing Process (Bold Text Indicates Local Failures)

Step	Live load (kN/m)	Node 8	
		Relative crack depth ξ	Compressive stress σ_c (MPa)
1	0.00	0.00	1.30
2	2.60	Crack initiation	11.80
3	2.80	**0.75**	**161.00**

Elastic, Plastic, Fracture Analysis of Masonry Arches

The study of the gradual transitions from an elastic stage to a damaged one for a masonry arch bridge is a prelude to the exploiting of the ultimate bearing capacity, established by means of limit analysis. Therefore, the fracturing benefit detected by the fracture analysis in comparison to the elastic analysis foreshadows the plastic benefit theorized by Heyman (1966). As an example, the masonry arch of the Fucine di Viù Bridge was considered, and for the purpose of computing the ultimate load following Heyman, the *ARCO* program (http://gelfi.unibs.it/arco.htm) developed by the University of Brescia (Italy) was used. This software is an analysis tool for masonry arches and vaults based on the safe theorem of the plastic analysis method (Heyman 1982).

Taking into account the aforementioned geometry, dead loads, and filling for the Fucine di Viù Bridge model, the increase of a uniformly distributed live load led to the thrust line remaining entirely

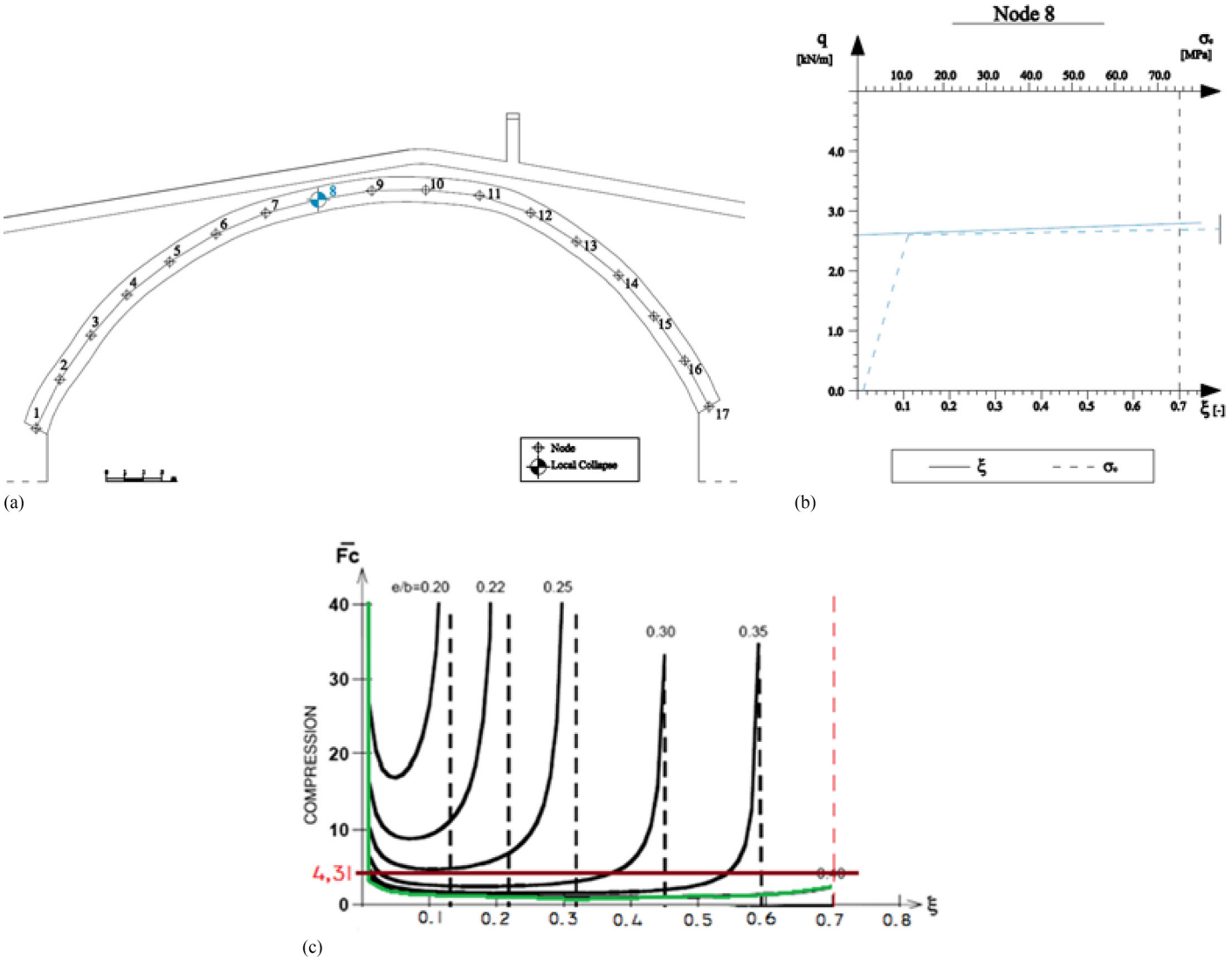

Fig. 14. Devil's Bridge: (a) damage localization; (b) local collapse; (c) snap-through

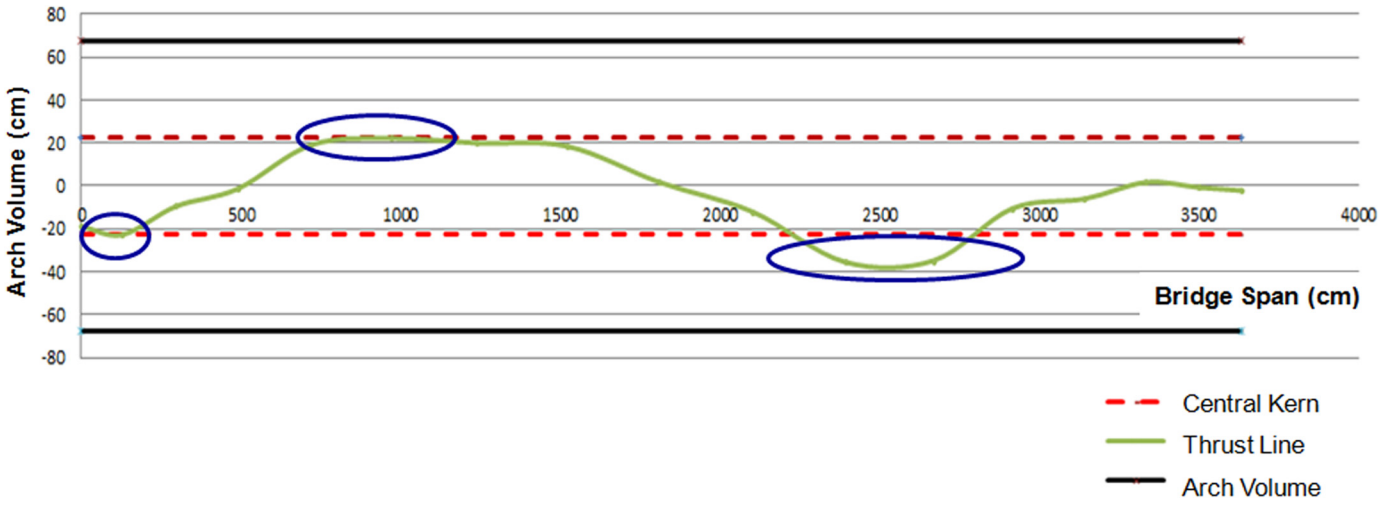

Fig. 15. Devil's Bridge analyzed by Mery's method, taking into account the dead load alone; to better appreciate the thrust-line trend, arch volume and central kern contours are rectified following Fuller's theory (adapted from Fuller 1875)

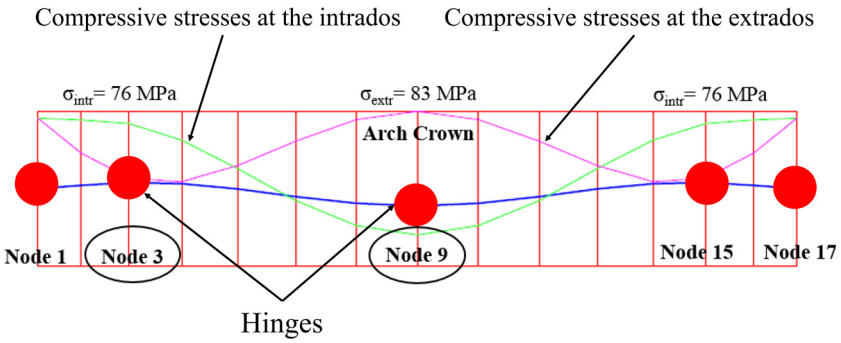

Fig. 16. Fucine di Viù Bridge plastic analysis, taking into account a uniformly distributed live load of approximately 13 kN/m arch volume is rectified to better appreciate the internal stress contours, and the collapsed cross sections are emphasized by the appearance of five hinges

within the arch volume. At least five points of crushing collapse (arch hinges) arose for a uniformly distributed live load of approximately 13 kN/m (Fig. 16). Note that two arch hinges (Nodes 3 and 9) were foreseen by the fracture analysis (see previous discussion), and the ratio plastic benefit/fracturing benefit was approximately 1.4, showing a gradual development in the structural analysis, taking into account fracture initiation, propagation, and the final appearance of the structure's ultimate bearing capacity.

Conclusions

A method is proposed that allows the capture of the arch-damaging process, which takes place when the conditions assessed through linear elastic analysis are no longer valid and before the set-in of the conditions established by means of limit analysis. The present approach can deeply analyze the gradual developments that take into account the fracture initiation and propagation occurring before the exploitation of the structure's ultimate bearing capacity.

After a short historical review of masonry arch bridge design, the evolutionary analysis of the fracturing process as applied to three medieval masonry arch bridges situated in the Lanzo Valleys (Italy) was presented. Through the proposed damage assessment, the present work shows how the arch behavior is affected by crack formation and by the internal stress redistribution, and it clarifies how the maximum admissible load evaluated by means of LEFM is larger than the load predicted by the theory of elasticity. Such an increase in terms of maximum admissible load can be defined as the fracturing benefit, and it is analogous to the plastic benefit of limit analysis. Therefore, the study of the transitions from an elastic stage to a damaged one returns an accurate and effective whole-service-life assessment of a masonry arch bridge.

Acknowledgments

The authors are grateful to Eng. Alessandro Lano for the collaboration in the analysis of the historical monuments.

References

Accornero, F., Lacidogna, G., and Carpinteri, A. (2016). "Evolutionary fracture analysis of masonry arches: Effects of shallowness ratio and size scale." *C.R. Mec.*, 344(9), 623–630.

ARCO [Computer software]. University of Brescia, Brescia, Italy.

Becchi, A., and Foce, F. (2002). *Degli archi e delle volte. Arte del costruire tra meccanica e stereotomia*, Marsilio, Venezia, Italy.

Benvenuto, E., and Radelet de Grave, P. (1995). *Between mechanics and architecture*, Birkhäuser, Basel, Switzerland.

Betti, M., Drosopoulos, G. A., and Stavroulakis, G. E. (2008). "Two nonlinear finite element models developed for the assessment of failure of masonry arches." *C.R. Mec.*, 336(1-2), 42–53.

Block, P., De Jong, M. J., and Ochsendorf, J. A. (2006). "As hangs the flexible line: Equilibrium of masonry arches." *Nexus Network J.*, 8(2), 13–24.

Boothby, T. E. (2001). "Analysis of masonry arches and vaults." *Prog. Struct. Eng. Mater.*, 3(3), 246–256.

Brencich, A., and Morbiducci, R. (2007). "Masonry arches: Historical rules and modern mechanics." *Int. J. Archit. Heritage*, 1(2), 165–189.

Carpinteri, A. (1982). "Application of fracture mechanics to concrete structures." *J. Struct. Div.*, 108(4), 833–848.

Carpinteri, A. (1989a). "Cusp catastrophe interpretation of fracture instability." *J. Mech. Phys. Solids*, 37(5), 567–582.

Carpinteri, A. (1989b). "Size effects on strength, toughness, and ductility." *J. Eng. Mech.*, 10.1061/(ASCE)0733-9399(1989)115:7(1375), 1375–1392.

Carpinteri, A., and Accornero, F. (2018). "Multiple snap-back instabilities in progressive microcracking coalescence." *Eng. Fract. Mech.*, 187, 272–281.

Carpinteri, A., and Carpinteri, An. (1982). "Softening and fracturing process in masonry arches." *Proc., 6th Int. Brick Masonry Conf.*, International Masonry Society, Whyteleafe, U.K, 502–510.

Carpinteri, A., Lacidogna, G., and Accornero, F. (2015). "Evolution of fracturing process in masonry arches." *J. Struct. Eng.*, 10.1061/(ASCE)ST.1943-541X.0001071, 04014132.

Casapulla, C. (2001). "Dry rigid block masonry: Safe solutions in presence of Coulomb friction." *WIT Trans. Built Environ.*, 55, 251–261.

Casapulla, C., and Argiento, L. U. (2016). "The comparative role of friction in local out-of-plane mechanisms of masonry buildings. Pushover analysis and experimental investigation." *Eng. Struct.*, 126, 158–173.

Castigliano, A. (1879). *Théorie de l'Equilibre des systèmes elastiques et ses applications*, A. F. Negro, Turin, Italy.

Cavallari-Murat, A. (1973). *Lungo la Stura di Lanzo*, Istituto Bancario San Paolo, Torino, Italy.

Cavicchi, A., and Gambarotta, L. (2007). "Lower bound limit analysis of masonry bridges including arch-fill interaction." *Eng. Struct.*, 29(11), 3002–3014.

Coulomb, C. (1773). *Mémoires de mathématique et de physisque présentés à l'Académie royale des sciences, et lus dans les assemblées*, Académie Royale des Sciences, Paris.

Couplet, C. A. (1731). *De la poussée des voutes*, Académie Royale des Sciences, Paris.

De La Hire, P. (1730). "Traité de mécanique, où l'on explique tout ce qui est necessaire dans la pratique des arts." *Mémoires de l'Académie Royale des Sciences*, 9, 1–333.

Drosopoulos, G. A., Stavroulakis, G. E., and Massalas, C. V. (2006). "Limit analysis of a single span masonry bridge with unilateral frictional contact interfaces." *Eng. Struct.*, 28(13), 1864–1873.

Fett, T. (2001). "Mixed mode stress intensity factor for partially opened cracks." *Int. J. Fract.*, 111(4), 67–72.

Fuller, G. (1875). "Curve of equilibrium for a rigid arch under vertical forces." *Minutes Proc. Inst. Civ. Eng.*, 40(1875), 143–149.

Gilbert, M., and Melbourne, C. (1994). "Rigid block analysis of masonry structures." *Struct. Eng.*, 72(21), 356–361.
Heyman, J. (1966). "The stone skeleton." *Int. J. Solids Struct.*, 2(2), 249–279.
Heyman, J. (1982). *The masonry arch*, Ellis Horwood, Chichester, U.K.
Heyman, J. (1998). *Structural analysis: A historical approach*, Cambridge University Press, Cambridge, U.K.
Hooke, R. (1675). *A description of helioscopes, and some other instruments*, T.R. for John Martyn, London.
Karnowsky, I. (2012). *Theory of arched structures*, Springer, New York.
Kooharian, A. (1953). "Limit analysis of voussoir (segmental) and concrete arches." *J. Am. Concr. Inst.*, 89, 317–328.
Lacidogna, G., and Accornero, F. (2018). "Elastic, plastic, fracture analysis of masonry arches: A multi-span bridge case study." *Curved Layered Struct.*, 5(1), 1–9.
Lacidogna, G., Accornero, F., Corrado, M., and Carpinteri, A. (2013). "Crushing and fracture energies in concrete specimens monitored by Acoustic Emission." *Proc., 8th Int. Conf. on Fracture Mechanics of Concrete and Concrete Structures*, FraMCos 2013, International Center for Numerical Methods in Engineering, Barcelona, Spain, 1726–1736.
Lourenço, P. (2000). "Anisotropic softening model for masonry plates and shells." *J. Struct.Eng.*, 10.1061/(ASCE)0733-9445(2000)126:9(1008), 1008–1015.
Mascheroni, L. (1785). *Nuove ricerche sull'Equilibrio delle volte*, Locatelli, Bergamo.
Mery, E. (1840). "Équilibre des voûtes en berceau." *Annales des Ponts et Chaussées*, 1, 50–70.
Milani, G., and Lourenço, P. B. (2012). "3D non-linear behavior of masonry arch bridges." *Comput. Struct.*, 110–111, 133–150.
Navier, C. L. (1833). *Résumé des leçons données à l'École des ponts et chaussées sur l'Application de la mécanique à l'Établissement des constructions et des machines*, Paris.
Orduña, A., and Lourenço, P. B. (2005). "Three-dimensional limit analysis of rigid blocks assemblages. Part I: Torsion failure on frictional interfaces and limit analysis formulation." *Int. J. Solids Struct.*, 42(18–19), 5140–5160.
Page, J. (1993). *Masonry arch bridges*, Her Majesty's Stationery Office, London.
Paradiso, M., Tempesta, G., Galassi, S., and Pugi, F. (2007). *Sistemi voltati in muratura*, DEI, Rome, Italy.
Pippard, A. J. S. (1948). "The approximate estimation of safe loads on masonry bridges." *The civil engineer in war: A symposium of paper on war-time engineering problems*, Thomas Telford, London, 365–372.
Poleni, G. (1748). *Memorie istoriche della gran cupola del tempio vaticano*, Stamperia del Seminario, Padova, Italy.
Poncelet, J. V. (1852). "Examen critique et historique des principales théories ou solutions concernant l'équilibre des voûtes." *C.R. Acad. Sci.*, 35, 494–587.
Tada, H., Paris, P. C., and Irwin, G. R. (1985). *The stress analysis of crack handbook*, Paris Productions, St. Louis.
Taylor, N., and Mallinder, P. (1993). "The brittle hinge in masonry arch mechanisms." *Struct. Eng.*, 71(20), 359–366.
Tóth, A. R., Orbán, Z., and Bagi, K. (2009). "Discrete element analysis of a stone masonry arch." *Mech. Res. Commun.*, 36(4), 469–480.
Vitruvius Pollio, M. (1914). *De Architectura*, Harvard University Press, Cambridge, MA.
Vittone, B. A. (1766). *Istruzioni diverse concernenti l'officio dell'Architetto civile*, Agnelli, Lugano, Switzerland.